



Contents lists available at ScienceDirect

American Journal of Transplantation

journal homepage: www.amjtransplant.org

Original Article

A new principle to attenuate ischemia-reperfusion injury in kidney transplantation



Ali-Reza Biglarnia^{1,†} , Yuji Teramura^{2,3,4,†} , Sana Asif² , Claudia Dührkop² , Vivek Anand Manivel² , Elin Manell⁵ , Patricia Hedenqvist⁵ , Anneli Rydén⁵ , Felix Sellberg² , Karin Fromell² , Sabine Hammer⁶ , Markus Huber-Lang⁷ , Kristina N. Ekdahl^{2,8} , Marianne Jensen-Waern^{5,‡} , Bo Nilsson^{2,‡,*} 

¹ Department of Surgery, Department of Clinical Sciences Malmö, University Hospital, Lund University, Malmö, Sweden

² Department of Immunology, Genetics, and Pathology (IGP), Rudbeck Laboratory C5:3, Uppsala University, Uppsala, Sweden

³ Cellular and Molecular Biotechnology Research Institute (CMB), National Institute of Advanced Industrial Science and Technology (AIST), Tsukuba, Ibaraki, Japan

⁴ Master's/Doctoral Program in Life Science Innovation (T-LSI), University of Tsukuba, Tsukuba, Ibaraki, Japan

⁵ Department of Clinical Sciences, Faculty of Veterinary Medicine and Animal Science, Swedish University of Agricultural Sciences, Uppsala, Sweden

⁶ Immunology, Department of Biological Sciences and Pathobiology, University of Veterinary Medicine Vienna, Vienna, Austria

⁷ Institute for Clinical and Experimental Trauma-Immunology, University Hospital of Ulm, Ulm, Germany

⁸ Linnæus Center of Biomaterials Chemistry, Linnæus University, Kalmar, Sweden

ARTICLE INFO

Keywords:

intravascular innate immunity
ischemia-reperfusion injury
kidney transplantation
pretreatment modality

ABSTRACT

Ischemia-reperfusion injury in transplantation remains a significant clinical challenge with regard to both short-term and long-term complications. In this study, we developed a new amphiphilic construct, polyethylene glycol (PEG)-conjugated lipids (PEG-LIPIDs), to be administered ex vivo intra-arterially to procured porcine kidney allografts before reperfusion. The aim was to create a protective cell membrane barrier, preventing the recognition of ligands exposed on renal cells by plasma proteins and cells of the intravascular innate immune system. In vitro cell studies confirmed the safety of PEG-LIPID with no observed toxicity and demonstrated its efficacy in masking ligands on various cell types. The PEG-LIPID was evaluated in 3 porcine allogeneic transplant models: 1 acute dual en bloc nonsurvival transplant model (duration 6 hours) and 2 survival models with low and high

Abbreviations: ANSM, acute nonsurvival model; biotin-PEG-LIPID, biotin-conjugated PEG-LIPID; CCRF-CEM, Caucasian acute lymphoblastic leukemia; CL-11, collectin-11; C1INH, C1 inhibitor; FAM-PEG-LIPID, fluorescein-labeled polyethylene glycol-conjugated lipid; FITC, fluorescein isothiocyanate; GCX, glycocalyx; HO-1, heme oxygenase-1; HTK, histidine-tryptophan-ketoglutarate; IL, interleukin; IRI, ischemia-reperfusion injury; MBL, mannan-binding lectin; NHS, N-hydroxy succinimide; PCR, polymerase chain reaction; PEG, polyethylene glycol; PEG-LIPID, polyethylene glycol-conjugated lipid; RBC, red blood cell; SLA, swine leukocyte antigen; SM, survival model; TAT, thrombin-antithrombin complex; TF, tissue factor; TNF, tumor necrosis factor; WIT, warm ischemic time; vWF, von Willebrand factor.

* Corresponding author. Dag Hammarskjölds väg 20, University Hospital, 751 85 Uppsala, Sweden.

E-mail address: bo.nilsson@igp.uu.se (B. Nilsson).

[†] These authors contributed equally: Ali-Reza Biglarnia and Yuji Teramura.

[‡] Marianne Jensen-Waern and Bo Nilsson contributed equally as senior authors.

<https://doi.org/10.1016/j.ajt.2025.08.024>

Received 17 June 2025; Received in revised form 27 July 2025; Accepted 17 August 2025

Available online 24 September 2025

1600-6135/© 2025 The Author(s). Published by Elsevier Inc. on behalf of American Society of Transplantation & American Society of Transplant Surgeons. This is an open access article under the CC BY license (<http://creativecommons.org/licenses/by/4.0/>).

ischemic stress, respectively (duration 96 hours). No immunosuppression was employed. Across all 3 porcine transplant models, PEG-LIPID consistently mitigated ischemia-reperfusion-induced thromboinflammation (complement, coagulation, and kallikrein/kinin activation) and long-term inflammation with a marked reduction in cytokine responses, including lower levels of interleukin 6. The PEG-LIPID-treated kidneys exhibited significantly improved allograft function, reflected in robustly lower creatinine levels. This translational study confirmed that the PEG-LIPID is a strong candidate drug to mitigate ischemia-reperfusion injury in clinical kidney transplantation.

1. Introduction

Ischemia-reperfusion injury (IRI) is a fundamental pathologic process contributing to tissue damage across diverse conditions, including trauma, stroke, and myocardial infarction.^{1,2} In organ transplantation, where IRI is inevitable, it contributes to early graft dysfunction and long-term failure.³ However, effective therapies remain limited.

The vascular endothelium and other blood-contacting cell surfaces are coated with a highly blood-compatible, negatively charged glycocalyx (GCX), comprising proteoglycans and glycosaminoglycans like hyaluronan and heparan sulfate.^{4,5} The GCX incorporates anticomplement and anticoagulant proteins, eg, C4b binding protein, factor H, C1 inhibitor (C1INH), anti-thrombin, protein C, and tissue factor (TF) pathway inhibitor⁶ that maintain microvascular homeostasis and prevent thromboinflammation. The GCX also shields adhesion molecules such as intercellular adhesion molecule-1, vascular cell adhesion molecule-1, and E-selectin on the endothelial cell surface, preventing leukocyte and platelet recruitment.⁶

A central mechanism of IRI is the degradation of the GCX through enzymatic cleavage by hyaluronidase, heparanase, and metalloproteinases.^{4,5} Due to this degradation, the protective properties of the GCX are lost, which subjects kidney cells to IRI-induced immune attacks during reperfusion of the graft. This initiates a rapid and interlinked activation of the complement, coagulation, and kallikrein-kinin systems—resulting in thromboinflammation.⁷

This cascade system activation is evidenced by the binding of complement components C3 and C4d, membrane attack complex deposition,⁸ and the involvement of lectin pathway components such as collectin-11 (CL-11)/-12, mannan-binding lectin (MBL), and MBL-associated serine protease-2.⁸⁻¹¹ Concurrent activation of TF and von Willebrand factor (vWF)¹² further promotes platelet adhesion and neutrophil activation on endothelial surfaces, culminating in thromboinflammation.⁷

In a recent clinical cohort study, we confirmed this mechanism in human kidney transplantation by measuring activation products from all 3 cascade systems in renal venous blood immediately after reperfusion. This revealed a rapid and interlinked activation of the complement, contact, and coagulation systems, culminating in a thromboinflammatory response that was significantly associated with both short- and mid-term (24-month) graft dysfunction.¹³

Inspired by these findings, we developed an innovative technique using an amphiphilic polymer—a polyethylene glycol (PEG)-conjugated lipid (PEG-LIPID), which spontaneously inserts into cell membranes to replace the GCX and mask surface antigens.^{14,15} The current study aimed to evaluate the efficacy and safety of PEG-LIPID for attenuating IRI-induced thromboinflammation through *in vitro* experiments and clinically relevant *in vivo* porcine kidney transplantation models (Fig. 1).

2. Materials and methods

2.1. Preparation of PEG-LIPID derivatives

PEG-phospholipid and maleimide-PEG-phospholipid (PEG-LIPID) were synthesized from PEG-N-hydroxysuccinimide (NHS) or NHS-PEG-Mal, and 1,2-dipalmitoyl-sn-glycero-3-phosphoethanolamine as described with slight modification.¹⁶ Fluorescein labeling was performed by conjugating 5-carboxy fluorescein to maleimide-PEG-phospholipid. Biotin-conjugated PEG-LIPID (biotin-PEG-LIPID) was synthesized by reacting biotin-PEG-NHS (5000 Da) with 1,2-dipalmitoyl-sn-glycero-3-phosphoethanolamine.

2.2. Hemocompatibility testing

Surface-modified and native mesenchymal stromal cells were exposed to whole human blood in a Chandler loop model.¹⁷

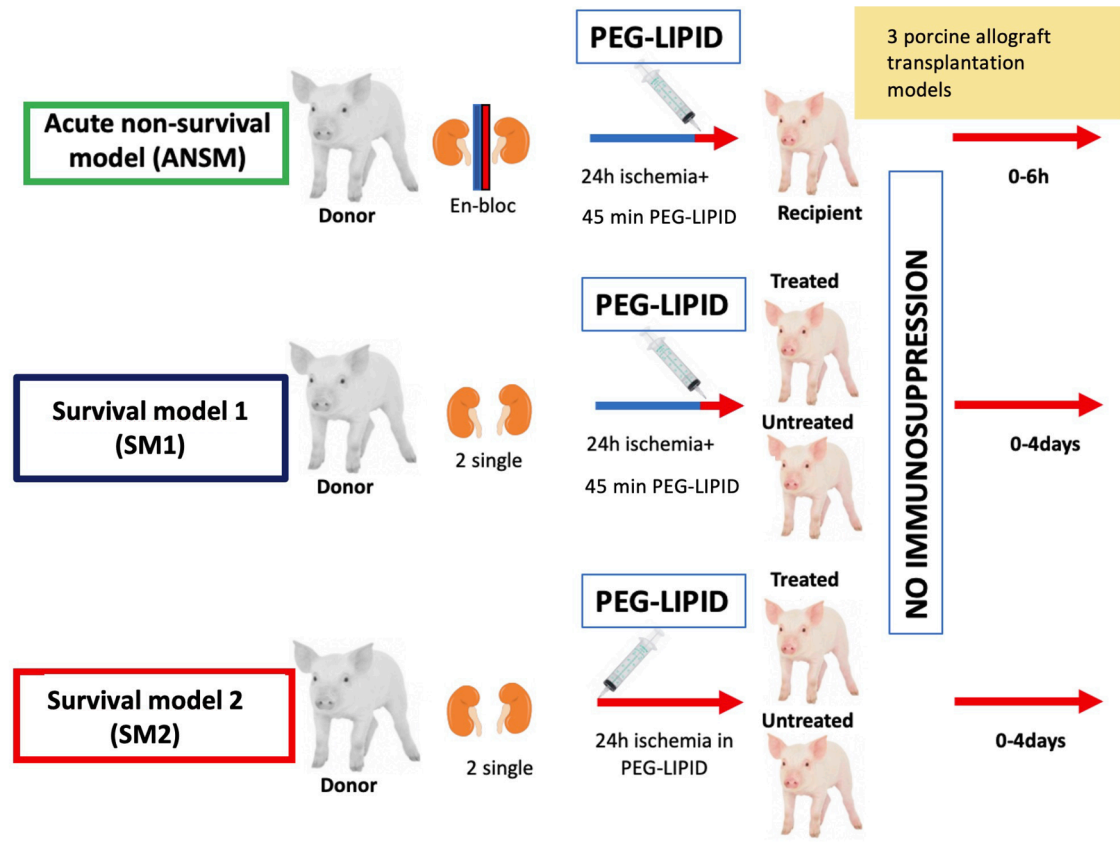
2.3. Coating and *in vitro* toxicity of PEG-LIPID

Caucasian acute lymphoblastic leukemia (CCRF-CEM) cells were coated with PEG-LIPID at room temperature. Toxicity was tested using commercial kits for proliferation, cell viability, ADP-ATP ratio, and Ca²⁺ flux.

2.4. Masking of antigens by PEG-LIPID on various cell types

PEG-LIPID coating was applied to 3 types of cells:

1. CCRF-CEM: Fluorescein isothiocyanate (FITC)-labeled anti-human CD52, anti-human CD4, or Alexa⁴⁸⁸-labeled anti-human CD8.
2. Human umbilical vein endothelial cells: FITC-labeled anti-CD31, anti-vWF. Plasma-exposed cells: FITC-labeled concanavalin A, anti-CL-11, and anti-MBL.



Study	Donors (n)	PEG-LIPID (n)	Controls (n)	Ischemia time	Dose/exposure	Sampling time/specimen
Acute non-survival model (ANSM)	6	6 <i>en bloc</i>	6 <i>en bloc</i>	WIT: < 5min CIT: 24h	5 mL (2mg/mL) 45min	1, 5, 15, 30, 60, 120, 240, 360min (graft vein) biopsy: 5, 60, 360min urine: 1, 6h
Allogeneic survival model 1 (SM1)	5	6	4	WIT: < 5min CIT: 24h	15mL (2mg/mL) 45min	5, 60min (graft vein) 24, 48, 72, 96h (systemic) biopsy: 5min, 96h
Allogeneic survival model 2 (SM2)	5	5	5	WIT: 0min CIT: 24h	250mL (2mg/mL) 24h	5, 15, 30, 60min (graft vein) 24, 48, 72, 96h (systemic)
Modified SM1 (detachment <i>in vivo</i>)	2	4	-	WIT: < 5min CIT: 24h	15mL (2mg/mL) 45min	biopsy: 0, 12, 24, 48, 72h

WIT: warm ischemia time; CIT: cold ischemia time.

Figure 1. Experimental outline. Three porcine allogeneic kidney transplant models were used for the evaluation of precoating of the graft with polyethylene glycol-conjugated lipid (PEG-LIPID). Acute nonsurvival model (ANSM): a dual en bloc nonsurvival transplant model (duration 6 hours). Survival model 1 (SM1) with high ischemic stress (duration 96 hours). Survival model 2 (SM2) with reduced ischemic stress (duration 96 hours). In each model, the PEG-LIPID is administered ex vivo by perfusion of the vascular tree of the kidney before reperfusion of the graft. No immunosuppression was used in either study. Upper panel: visual overview of the transplantation models. Lower panel: quantitative information on numbers of donors and recipients, ischemia time, dose of administered PEG-LIPID, and time points for sampling of different specimens.

- Human red blood cells: Alexa⁴⁸⁸-labeled anti-blood group B antigen antibody. Complement-mediated lysis (A481 nm) was analyzed after incubation of red blood cells (RBCs) in ABO-incompatible serum. Masking of the RhD blood group antigen was measured using agglutination, and all other samples were measured using flow cytometry.

2.5. Analyses of plasma, kidney biopsies, and urine

Plasma samples stored at -80°C were analyzed for complement activation markers (C3a, sC5b-9¹⁸; Antibodies [online.com](#)), coagulation markers (thrombin-antithrombin complex [TAT]), and FXIIa-C1INH complexes using enzyme-linked immunosorbent assay (Enzyme Research Laboratories, South Bend, IN, USA) and cytokines using multiplex Luminex xMAP Technology (Millipore Corporation, MA, USA) or enzyme-linked immunosorbent assay (Gyros, Uppsala, Sweden), as well as for creatinine levels.

Kidney biopsies were subjected to immunohistochemical analyses using an alkaline phosphatase-based system followed by counterstaining with hematoxylin. Antibodies to C3b, C4d, membrane attack complex, nitrotyrosine, heme oxygenase-1 (HO-1), and nitric oxide synthase-2 were used. Expression of tumor necrosis factor (TNF), interleukin (IL)-1 β , IL-6, and TF was assessed using real-time polymerase chain reaction (PCR).

Urine samples were collected in the acute nonsurvival model (ANSM) from both kidneys, separately catheterized for 6 hours. The urine was analyzed for fluorescein-labeled PEG-LIPID (FAM-PEG-LIPID) in a fluorescence plate reader.

2.6. Determination of the saturating binding concentration of PEG-LIPID in porcine kidney grafts

Kidneys were procured from anesthetized pigs. Kidneys were either manually perfused *ex vivo* with 100, 250, or 500 mL of FAM-PEG-LIPID (2 mg/mL in histidine-tryptophan-ketoglutarate [HTK]) followed by incubation for 45 minutes or perfused with FAM-PEG-LIPID by machine perfusion (LifePort Kidney Transporter; Organ Recovery Systems) for 60 minutes. Fluorescence was measured using a fluorescence plate reader (excitation wavelength of 485 nm/emission wavelength of 528 nm).

2.7. Three porcine allogeneic transplantation models

To study the effects of the *ex vivo* allograft coating with PEG-LIPID in porcine allogeneic transplantation, 3 different transplant models were used: a dual en bloc, acute nonsurvival model (ANSM) (green frames), and 2 single graft allogeneic survival models (SMs), SM1 (blue frames) with high and SM2 (red frames) with reduced ischemic stress, respectively (Fig. 1). General management and treatment of the animals followed routines previously described.¹⁹ Reporting of the data is according to ARRIVE 2.0 essentials guidelines. All procedures were performed by the same transplantation team. The study was approved by the Ethics Committee for Animal Experimentation, Uppsala, Sweden (DnrC175/12 and DnrC123/14).

2.8. ANSM

Six donor pigs underwent en bloc kidney recovery following 3 to 5 minutes of *in situ* clamping (warm ischemic time [WIT]), followed by cold perfusion with HTK solution and cold storage at $+4^{\circ}\text{C}$ for 24 hours. After preservation, the arteries and corresponding veins of each kidney were carefully clamped. One kidney from each en bloc package was randomly selected and treated with 5 mL PEG-LIPID (2 mg/mL) via a single injection through the renal artery, followed by immediate clamping to avoid cross-contamination. After a minimum of 45 minutes of incubation at 4°C , the pigs underwent dual en bloc kidney transplantation. Postreperfusion, consecutive blood samples were collected from the renal veins at specified intervals up to 360 minutes. Biopsies were taken 5, 60, and 360 minutes postreperfusion (Fig. 1).

2.9. SMs (SM1 and SM2)

In SM1, following a 3- to 5-minute *in situ* WIT, kidneys were recovered en bloc, perfused with cold HTK on the bench, separated, and randomly assigned to either the control or the treatment group. The kidneys were then cold-stored at $+4^{\circ}\text{C}$ for 24 hours. Postpreservation, kidneys received either 15 mL PEG-LIPID (2 mg/mL) or HTK via arterial injection as specified for ANSM, followed by a minimum 45-minute incubation before reperfusion. Each kidney was subsequently transplanted separately into an individual recipient pig, with a bilateral native nephrectomy performed at the end of the procedure.

In SM2, kidneys were recovered en bloc after *in situ* cold perfusion with HTK, ensuring no WIT. On the bench, they were separated and assigned to either the control or treatment group. Unlike ANSM and SM1, kidneys in SM2 were treated before preservation through arterial infusion of 250 mL of either PEG-LIPID (2 mg/mL) or HTK, then submerged in the respective solution and cold-stored at $+4^{\circ}\text{C}$ for 24 hours. Postpreservation, each kidney was transplanted separately into an individual recipient pig, with a bilateral native nephrectomy performed at the end of the procedure.

In both models, blood samples were collected from renal veins at specified intervals postreperfusion and systemically up to 4 days posttransplant. Kidney biopsies were taken prereperfusion and at defined time points postreperfusion (Fig. 1). In SM2, 1 pig in the treatment group was excluded due to vascular malformation.

2.10. Swine leukocyte antigen typing using PCR with sequence-specific primers

In SM1, swine leukocyte antigen (SLA) typing was performed with the complete set of primers specific for the alleles at 3 SLA class I loci and 3 SLA class II loci,²⁰⁻²² to enable matching between the 2 recipients of kidneys from each donor.

2.11. *In vivo* pharmacokinetics

In vivo detachment kinetics and half-life of biotin-labeled PEG-LIPID were studied in kidney biopsies and transplanted kidneys by a modification of SM1. Four recipient pigs were

transplanted with biotin-PEG-LIPID-treated kidneys and euthanized after 12, 24, 48, and 72 hours, respectively, and wedge biopsies were taken. The tissue sections containing biotin-labeled PEG-LIPID were treated with Alexa⁴⁸⁸-streptavidin (GE Healthcare, Uppsala, Sweden) and analyzed using fluorescence microscopy.

2.12. Statistical analyses

The statistical analyses were performed using Prism macOS Version 9.4.1 (458). One-sample, unpaired, paired, and multiple unpaired *t*-tests are used as indicated in the legends. In addition, 1-way analysis of variance and 2-way repeated measures analysis

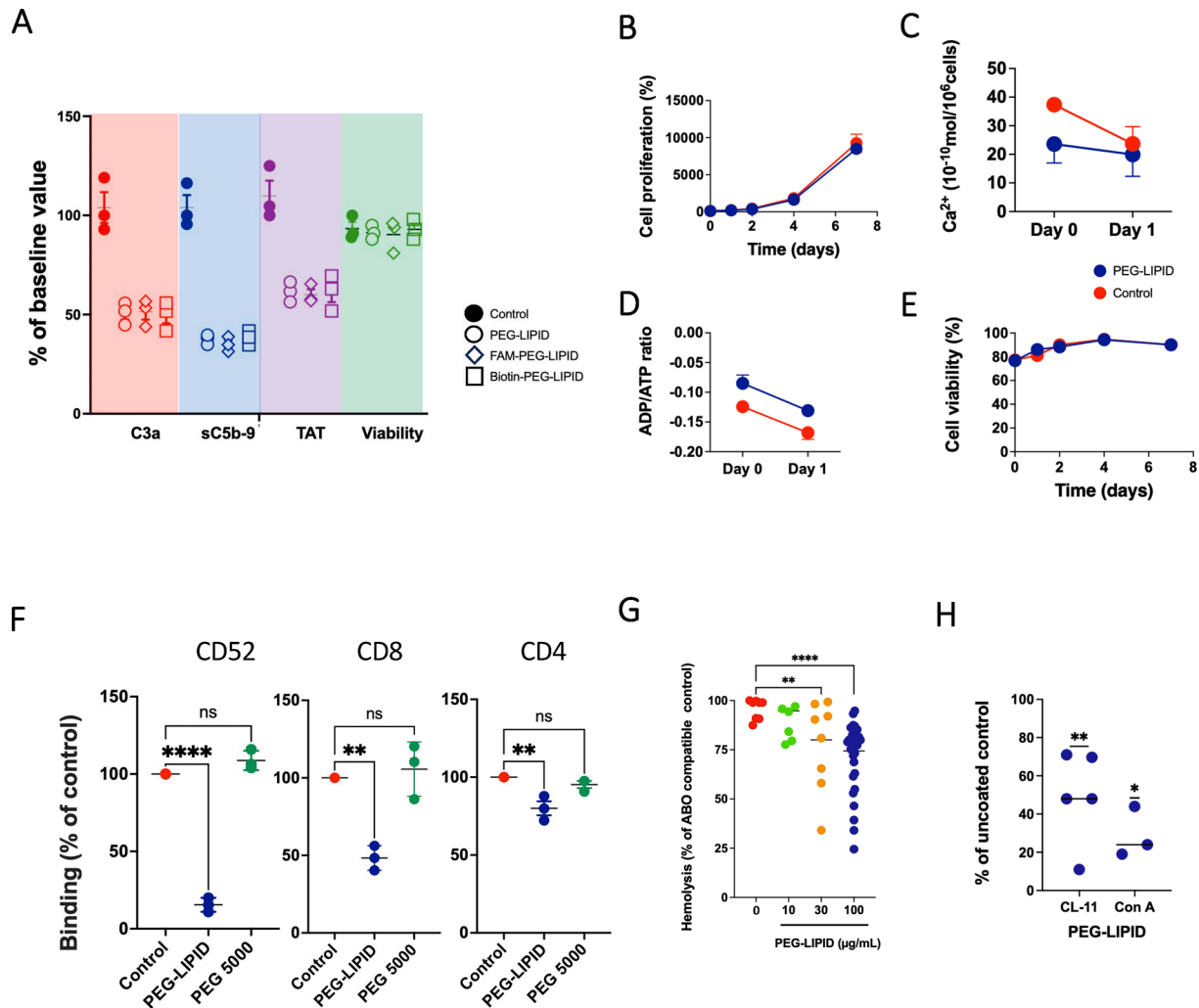


Figure 2. Effect of polyethylene glycol-conjugated lipid (PEG-LIPID) treatment in vitro and mechanism of action. (A) Protection against innate immunity by PEG-LIPID. A total of 3 million human mesenchymal stromal cells (MSCs) were incubated with 50 μ L of PEG-LIPID (2 mg/mL) for 30 minutes at room temperature. Three different PEG-LIPID preparations (PEG-LIPID, fluorescein-labeled PEG-LIPID [FAM-PEG-LIPID], and biotin-conjugated PEG-LIPID [biotin-PEG-LIPID]) used in this study were compared for their ability to attenuate innate immune reactions in human blood. The PEG-LIPID-coated (open symbols) and untreated cells (filled symbols) were incubated in 7 mL of fresh whole human blood at 37 $^{\circ}$ C for 60 minutes, and the concentrations of C3a, sC5b-9, and thrombin-antithrombin complex (TAT) were measured. The viability of the cells was also analyzed after 6 hours in cell culture ($n = 3$). Statistical evaluation using 1-way analysis of variance (ANOVA). (B-E) In vitro toxicity of PEG-LIPID. A total of 3 million Caucasian acute lymphoblastic leukemia (CCRF-CEM) cells were incubated with 50 μ L of PEG-LIPID (2 mg/mL) for 30 minutes at room temperature, followed by culture for up to 7 days and analyzed regarding (B) proliferation, (C) Ca²⁺ flux, (D) ADP-ATP ratio, and (E) cell viability ($n = 3$ for each assay). (B, E) Cell growth and cell viability were assessed using the trypan blue exclusion test and cell counting at baseline and 1, 2, 4, and 7 days. (C, D) Intracellular Ca²⁺ concentration and the ADP-ATP ratio were measured after 1 and 24 hours of culture as cytotoxicity assays to evaluate general cellular processes such as apoptosis, necrosis, and proliferation. The results from (B-E) demonstrate that PEG-LIPID has no toxic effects on cells in vitro, as no significant differences were observed between PEG-LIPID-treated and untreated cells ($n = 3$). (F) Coating of CCRF-CEM cells with PEG-LIPID, but not with free PEG 5000, inhibited the binding of monoclonal antibodies (mAbs) to surface antigens CD52, CD8, and CD4 to varying degrees, as analyzed using flow cytometry ($n = 3$). (G) Red blood cell (RBC) coated with PEG-LIPID and incubated with ABO-mismatched serum exhibited reduced complement-mediated lysis (right panel, $n = 13$). (H) The binding of the lectin pathway (LP) recognition molecule collectin-11 (CL-11) ($n = 5$) to native and PEG-LIPID-coated human umbilical vein endothelial cells (HUVECs) after exposure to human plasma was analyzed using flow cytometry. The CL-11 binding is presented after subtracting the binding observed in the presence of 10 mM EDTA. The binding of concanavalin A (Con A), a lectin with broad specificity, to HUVECs without plasma exposure was also assessed ($n = 3$). Results demonstrated that the PEG-LIPID coating effectively masked acceptor molecules for both Con A and, to a varying degree, CL-11.

of variance followed by multiple comparisons testing without (in figure 5 panels E and F) and with (all other panels) Bonferroni correction, were used. The results are presented as mean \pm SEM (ns, $P \leq .05$, $P < .01$, $P < .001$, and $P < .0001$).

3. Results

3.1. In vitro studies on the metabolic effects, efficacy, and mechanism of action of PEG-LIPID coatings

3.1.1. The functional effect of nonlabeled and labeled PEG-LIPID

Three different PEG-LIPID preparations were utilized in this study: nonconjugated PEG-LIPID, FAM-PEG-LIPID, and biotin-PEG-LIPID. Their effects on thromboinflammation and cell viability were assessed using mesenchymal stromal cells in a whole human blood model. C3a, sC5b-9, and TAT, and their viability was found to be similar across all preparations (Fig. 2A), confirming that the modifications did not alter the efficacy of the PEG-LIPID formulations.

3.1.2. Toxic and metabolic effects of cell-bound PEG-LIPID

Side effects of cell-bound PEG-LIPID were investigated using in vitro experiments on CCRF-CEM. The study assessed several key parameters, including cell proliferation rate (Fig. 2B), calcium flux (Ca^{2+} flux, Fig. 2C), ADP-ATP ratio (Fig. 2D), and cell viability via the trypan blue exclusion assay (Fig. 2E). Results showed no significant differences in these cellular functions.

3.1.3. Mechanism of action

The effect of the PEG-LIPID coating on antibody and plasma protein binding to various surface antigens/ligands reaching out distinctively differently from the surface was investigated. First, the binding of FITC-labeled monoclonal antibodies directed against the 3 different surface antigens, CD52 (1 nm), CD8 (5-10 nm), and CD4 (15 nm), on PEG-LIPID-coated CCRF-CEM cells was assessed by flow cytometry (Fig. 2F). The PEG-LIPID inhibited monoclonal antibody binding to CD52 almost completely; binding to CD8 was reduced by half, whereas binding to CD4 was only marginally affected. Free PEG and phosphate-buffered saline had no effect. Human RBCs of blood type B were treated with PEG-LIPID, and the binding of FITC-labeled anti-blood group B antigen antibodies was analyzed using flow cytometry. The results showed that PEG-LIPID treatment significantly reduced antibody binding. This reduction was further supported by a dose-dependent decrease in complement-mediated lysis of the RBCs (Fig. 2G). Additionally, we determined whether PEG-LIPID coating could reduce the binding of collectin-11 (CL-11), a molecule that binds to fucose (5 nm) and is implicated in IRI, and concanavalin A (Con A; a lectin) to human umbilical vein endothelial cells. In both scenarios, PEG-LIPID treatment substantially reduced binding (Fig. 2H). All masking experiments are summarized in Table 1.²³⁻²⁸

3.2. Distribution and pharmacokinetics of the PEG-LIPID in vitro and in vivo

3.2.1. Determination of the saturating binding concentration of PEG-LIPID in kidney grafts

Saturation was found at concentrations exceeding 0.5 mg/mL FAM-PEG-LIPID and 30 min incubation time at room temperature (Fig. 3A). By perfusing porcine kidneys ex vivo with increasing volumes of compound (2 mg/mL), the maximum saturating binding was reached already between 0.2 and 0.3 mg/g of kidney tissue using 100 and 250 mL. Larger volumes (500 mL) significantly increased nonbound FAM-PEG-LIPID in the urine (urinary secretion and retention within the renal pelvis) (Fig. 3B, Table 2). Employing hypothermic machine perfusion, these data were confirmed (0.3 mg/g of kidney tissue; Fig. 3C).

3.2.2. Microscopic distribution of PEG-LIPID in kidney tissue

Microscopic imaging was performed on in vivo wedge biopsies of porcine kidneys treated with biotin-PEG-LIPID post-reperfusion, taken in vivo from the ANSM experiments (Fig. 3D). The analysis revealed that biotin-PEG-LIPID was uniformly

Table 1

Masking of antigens by polyethylene glycol-conjugated lipid on various cell types.

Membrane proteins/ligands	Approx size (nm)	Inhibition by PEG-LIPID
CCRF-CEM cell line		
CD52; CAMPATH-1	1-3 nm ²⁸	High
CD8 ^a	5-10 nm ²⁴	Intermediate
CD4	15 nm ²⁵	Low
HUVECs		
CD31; PECAM-1	15 nm ²⁶	Low
vWF	>100 μm (multimer) ²⁷	Low
HUVECs plasma-treated		
Concanavalin A ^b	1-3 nm	Intermediate
CL-11 ^c	1-3 nm	Intermediate
MBL ^b	1-3 nm	Intermediate
RBC		
Blood group B antigen ^d	1-3 nm	High (>90%)
Rh D, C, c, E, e (gel cards)	1-3 nm ²³	High

CCRF-CEM, Caucasian acute lymphoblastic leukemia; CL-11, collectin-11; HUVEC, human umbilical vein endothelial cell; MBL, mannan-binding lectin; PECAM-1, platelet endothelial cell adhesion molecule-1; PEG-LIPID, polyethylene glycol-conjugated lipid; RBC, red blood cell; vWF, von Willebrand factor.

^a MW 21 to 28 kDa.

^b Targets multiple cell membrane carbohydrates.

^c Targets cell membrane fucose.

^d Cell membrane carbohydrate.

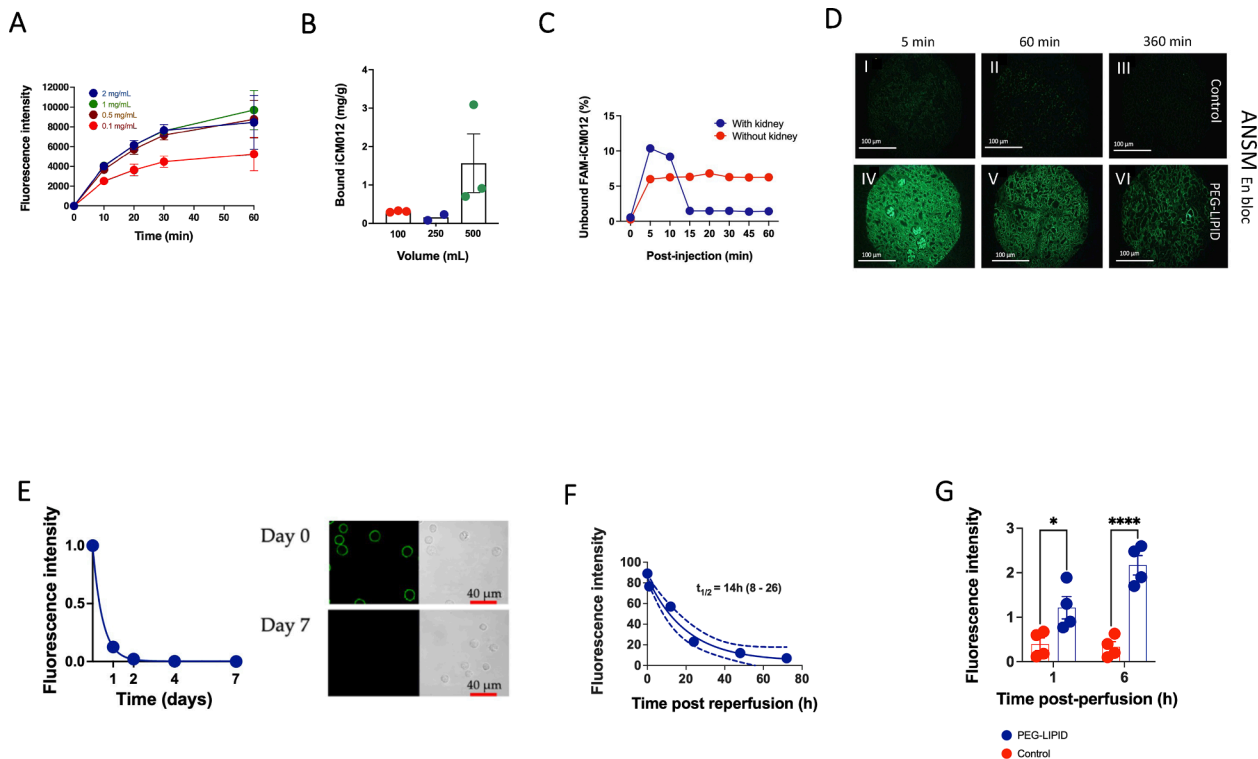


Figure 3. In vitro and in vivo pharmacokinetics of polyethylene glycol-conjugated lipid (PEG-LIPID). (A) Binding of fluorescein-labeled PEG-LIPID (FAM-PEG-LIPID) to cells in vitro. The kinetics of PEG-LIPID binding to cells were analyzed in vitro. Five million Caucasian acute lymphoblastic leukemia (CCRF-CEM) cells were incubated with 100 μL of FAM-PEG-LIPID (0.1–2 mg/mL) or phosphate-buffered saline (PBS; control) for 10 to 60 minutes at room temperature ($n = 3$). After washing, the bound FAM-PEG-LIPID was quantified using flow cytometry. PEG-LIPID binding was found to saturate at concentrations exceeding 0.5 mg/mL FAM-PEG-LIPID and a 30-minute incubation time. (B) Amount of bound FAM-PEG-LIPID at saturation in kidney tissue. Kidneys were procured from anesthetized pigs. The kidneys were perfused with 100, 250, or 500 mL of FAM-PEG-LIPID (2 mg/mL in histidine-tryptophan-ketoglutarate [HTK]) ex vivo and incubated for 45 minutes. After washing, the amount of FAM-PEG-LIPID in biopsies from kidney tissue and samples from secreted urine and from the pelvis was quantified using fluorescence. The saturating binding concentration of bound FAM-PEG-LIPID was calculated to be 0.2 to 0.3 mg/g kidney tissue. (C) Calculated amount of bound FAM-PEG-LIPID at saturation in kidney tissue using machine perfusion. The porcine kidneys were perfused with FAM-PEG-LIPID (2 mg/mL) using machine perfusion for 60 minutes. Machine perfusion circuits without connected kidneys were used as controls. The amount of FAM-PEG-LIPID in biopsies from kidney tissue and the perfusion fluid was quantified using fluorescence. The saturating binding concentration of bound FAM-PEG-LIPID was calculated to be approximately 0.3 mg/g kidney tissue. (D) Fluorescence imaging of a kidney perfused with FAM-PEG-LIPID in the acute nonsurvival model (ANSM): fluorescence imaging of a representative kidney perfused with FAM-PEG-LIPID in ANSM after 5 minutes revealed fluorescence, particularly in the glomeruli, as well as in the vasculature and tubules (left panel; IV). After 60 minutes, fluorescence in the glomeruli had largely disappeared but remained in both the vasculature and tubules (middle panel; V). By 360 minutes, fluorescence intensity had diminished further but maintained a similar distribution pattern (right panel; VI). No detectable fluorescence (ie, leakage from the treated kidney) was observed in the control kidney (upper panels; I, II, and III). (E) Detachment of PEG-LIPID from cells. Three million CCRF-CEM cells were incubated with 50 μL of FAM-PEG-LIPID (2 mg/mL) for 30 minutes at room temperature ($n = 3$). After washing, the cells were cultivated for 7 days, and the bound amount of PEG-LIPID was assessed using flow cytometry (left panel) and confocal microscopy (right panel). (F) Pharmacokinetics of PEG-LIPID in vivo. Two donor pigs underwent bilateral nephrectomy. The kidneys were then procured and kept in cold storage for 24 hours. Biotin-labeled PEG-LIPID was administered and incubated in both kidneys for 45 minutes. Thereafter, nonbound biotin-conjugated PEG-LIPID (biotin-PEG-LIPID) was flushed through the vascular system, and the kidneys were transplanted to recipient pigs, and initial biopsies were taken from the treated and native kidneys at transplantation and after 60 minutes ($n = 4$). Pigs were euthanized sequentially after 12, 24, 48, and 72 hours, and biopsies were taken from the transplanted and autologous kidneys. Fluorescence was detected using secondary Alexa⁴⁸⁸-streptavidin and confocal microscopy. To estimate the systemic leakage of PEG-LIPID, the autologous kidneys of the recipient were preserved and analyzed. It was shown to be very low, reliably detected only after 1 hour. The half-life of PEG-LIPID was calculated from fluorescence images, a 1-phase exponential decay model was applied to fit a curve to the data points, and $t_{1/2}$ was calculated to be 14 hours (95% confidence interval, 8–26). (G) Detection of fluorescence in the urine of 4 of the FAM-PEG-LIPID-treated and control kidneys in the ANSM, corroborating that the PEG-LIPID is at least to some degree excreted by the kidneys. Two-way repeated measure analysis of variance (ANOVA, coated/uncoated).

distributed across all cell types within the renal parenchyma as early as 5 minutes after reperfusion, with a preferential accumulation in the glomeruli. By 60 minutes, the distribution had equilibrated across the glomeruli, vessels, and tubules. After 360 minutes, a similar but weaker staining pattern was observed.

3.2.3. Detachment and half-life of PEG-LIPID in vitro and in vivo

The detachment of PEG-LIPID in vitro was analyzed by cultivating CCRF-CEM cells labeled with FAM-PEG-LIPID for 7 days and then assessing the amount of remaining PEG-LIPID

Table 2

Total bound FAM-PEG-LIPID, kidney weight pre-infusion and calculated binding in each experiment.

	Perfusion volume	Sample (n)			Mean
		1	2	3	
Total bound (mg)	100 mL	28.8	31.9	27.7	29.5
Weight (g)		86	102	95	94
Binding (mg/g)		0.33	0.31	0.29	0.31
Total bound (mg)	250 mL	28.1	9.0		18.5
Weight (g)		120	119		120
Binding (mg/g)		0.23	0.08		0.16
Total bound (mg)	500 mL	9.4	26.5	68.0	141.0
Weight (g)		102	85	97	95
Binding (mg/g)		0.91	3.09	0.70	1.6

using flow cytometry (left) and confocal microscopy (right) (Fig. 3E).

The kinetics of PEG-LIPID attached to the kidney parenchyma in vivo were studied in the porcine survival model (modified SM1; see below), where pigs were transplanted with grafts treated with biotin-PEG-LIPID ex vivo. From the fluorescence analysis using confocal microscopy visualized with Alexa⁴⁸⁸-streptavidin, a half-life of PEG-LIPID attached to the kidney parenchyma of approximately 14 hours was calculated (Fig. 3F). FAM-PEG-LIPID was consistently found in the urine in the ANSM (Fig. 3G).

3.3. PEG-LIPID-mediated attenuation of IRI

3.3.1. PEG-LIPID-mediated attenuation of IRI in 3 porcine transplantation models

To evaluate ischemic damage in the ANSM biopsies from PEG-LIPID-treated and control kidneys, which were collected after 5, 60, and 360 minutes postreperfusion and stained for nitrotyrosine, HO-1, and inducible nitric oxide synthase. No differences were observed between the treated and nontreated kidneys, indicating that both tissues were in a similar ischemic condition (Fig. 4A).

Furthermore, biomarkers of thromboinflammation in plasma samples collected from the renal veins of each kidney within the same en bloc package were analyzed. Complement (C3a and sC5b-9), coagulation (TAT), and contact system (FXIIa-C1INH) markers were found to be substantially lower in the treated kidneys compared to the untreated ones throughout the entire observation period of 360 minutes (Fig. 4B). Biopsies taken at 5 minutes revealed local deposition of complement fragments C4d and C3b. A significantly lower binding of C3b was observed in the PEG-LIPID-treated kidneys, with a tendency for a lower C4d binding as well (Fig. 4C).

Following reperfusion in the SM1, the levels of C3a, sC5b-9, and TAT in the plasma were substantially lower throughout the entire observation period (up to 4 days posttransplant) in animals receiving PEG-LIPID-treated kidneys (Fig. 4D). Renal

biopsies taken at 5 minutes postreperfusion and at necropsy on day 4 also demonstrated a lower binding of C3b in the PEG-LIPID-treated kidneys (Fig. 4E). Similar differences between the groups were found in the SM2 (Fig. 4F).

3.3.2. PEG-LIPID-mediated attenuation of systemic inflammation induced by ischemia reperfusion in 2 porcine transplantation models

In the ANSM, both the messenger RNA expression in kidney biopsies (real-time PCR, Fig. 5A) and the plasma concentration in the renal vein (Fig. 5B) of proinflammatory cytokines (TNF, IL-1 β , and IL-6) and TF were lower in the PEG-LIPID-treated animals compared to their respective controls. Notably, the IL-6 level was markedly suppressed at most time points.

In the SM1, proinflammatory cytokines reflecting local inflammation were assessed at 5 and 60 minutes postreperfusion, whereas systemic inflammation was evaluated 4 days posttransplant (Fig. 5C). An inflammatory response, though not statistically significant, was observed after only 5 minutes in untreated kidneys. By 60 minutes, this response had resolved, reaching a steady state. Four days later, a pronounced response engaging most of the analyzed cytokines, except for IL-8, was observed specifically in the pigs transplanted with untreated kidneys, demonstrating that PEG-LIPID treatment effectively attenuates systemic inflammation 4 days posttransplant. Similar differences between the groups were seen in the SM2 (Fig. 5D). Considering the short duration of the PEG-LIPID coating, the evidence suggests that PEG-LIPID-mediated inhibition of instantaneous thromboinflammation triggered by IRI also impacts long-term systemic inflammation.

No toxicity or safety concerns were observed in either transplantation model. This includes no differences in clinical parameters, laboratory results, pathology findings, general histology (hematoxylin staining), or macroscopic appearance between treated and untreated kidneys.

3.3.3. Functional effects of ex vivo PEG-LIPID treatment in porcine transplantation models

Kidney function was evaluated by measuring creatinine levels over time in blood samples collected from recipients in SM1 and SM2. Creatinine levels were found to be significantly lower posttransplant in pigs receiving PEG-LIPID-treated allografts compared with controls, with a more pronounced effect in the SM2 (Fig. 5E, F).

4. Discussion

Attempts to attenuate IRI using substances that target individual components of the intravascular innate immune system, such as anticomplement inhibitors,²⁹ have shown promise but remain inconclusive. As demonstrated by Strandberg et al,¹³ this is likely because IRI is driven by a complex interplay between plasma proteins, cascade systems, immune cells in the blood, and cells within the kidney allograft. Here, we introduced a novel strategy utilizing an amphiphilic polymer that spontaneously integrates into the cell membrane when administered ex vivo via a

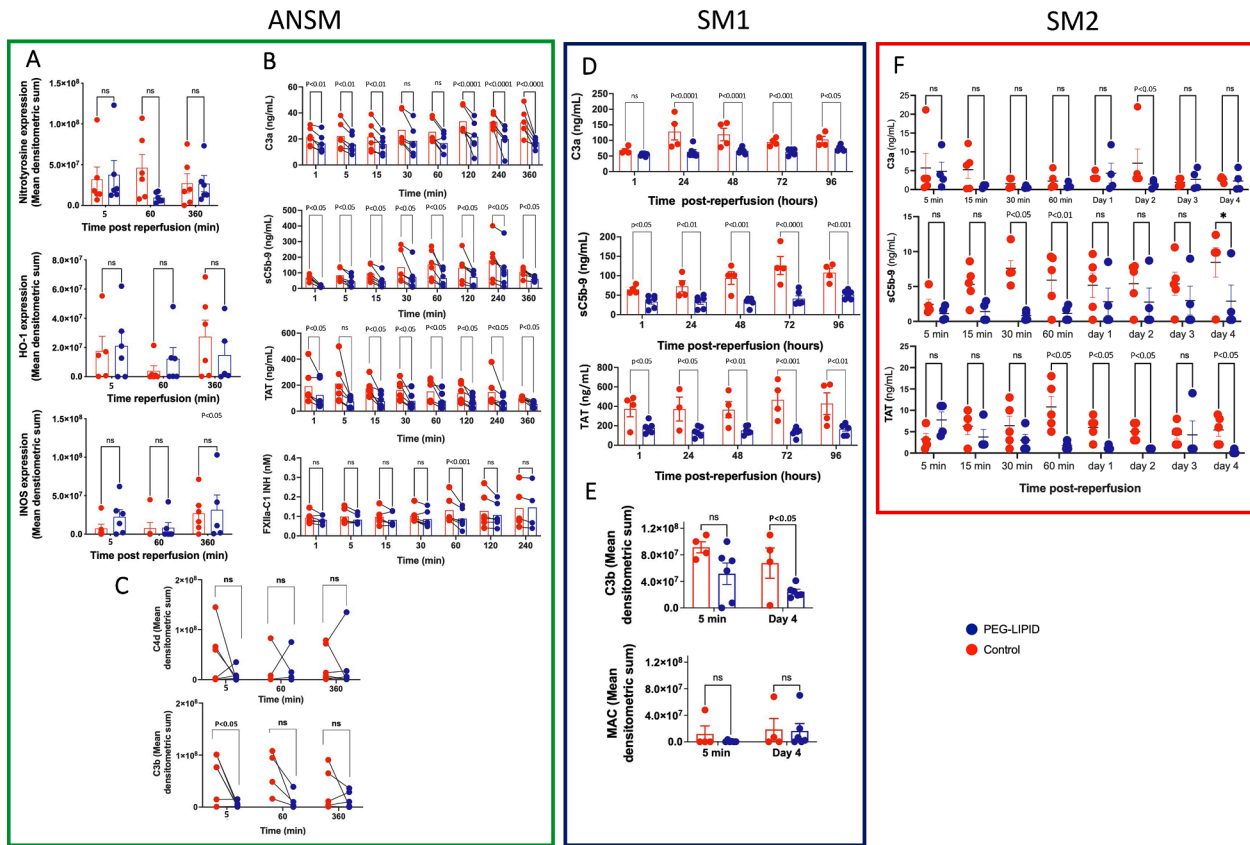


Figure 4. Ischemia-induced thromboinflammation in the porcine transplantation models. (A) The state of ischemia in polyethylene glycol-conjugated lipid (PEG-LIPID)-treated and nontreated kidneys in the acute nonsurvival model (ANSM): wedge biopsies were collected at 5, 60, and 360 minutes and analyzed immunohistochemically using confocal microscopy for protein expression of nitrotyrosine, heme oxygenase-1 (HO-1), and inducible nitric oxide synthase (iNOS). No significant differences were observed between treated and nontreated tissues, indicating no detectable difference in ischemic conditions. (B) Cascade system activation in the ANSM: markers of cascade system activation, including complement (C3a and sC5b-9), coagulation (thrombin-antithrombin complex [TAT]), and the contact system (FXIIa-C1INH), were measured in plasma serially sampled from the kidney vein of PEG-LIPID-treated kidneys and their controls during 360 minutes. (C) Deposition of thromboinflammation markers in the ANSM: wedge biopsies were collected at 5, 60, and 360 minutes and analyzed immunohistochemically for C4d and C3b deposition. (n = 6). (D) Cascade system activation in the SM1: markers for complement (C3a and sC5b-9) and coagulation (TAT) markers, as indicators of thromboinflammation, were measured in plasma sampled from the kidney vein of PEG-LIPID-treated kidneys and their controls at 60 minutes, followed by systemic sampling at 24, 48, 72, and 96 hours. (E) Deposition of thromboinflammation markers in the SM1: wedge biopsies were collected at 5 minutes and after 96 hours and analyzed immunohistochemically for C3b and membrane attack complex (MAC) deposition. (n = 6 treatments + 4 controls). (F) Cascade system activation in the SM2: markers for complement (C3a and sC5b-9) and coagulation (TAT) markers, as indicators of thromboinflammation, were measured in plasma sampled from the kidney vein of PEG-LIPID-treated kidneys and their controls for up to 60 minutes, followed by systemic sampling at 24, 48, 72, and 96 hours. (n = 5 treated + 5 controls). In summary, a significantly lower level of acute thromboinflammation was observed in both the ANSM and SM1 models, reflecting an attenuated ischemia-reperfusion injury (IRI). A similar trend was also seen in the less harsh SM2 model. Two-way repeated measure analysis of variance (ANOVA, coated/uncoated).

single arterial infusion to a recovered kidney allograft. This polymer forms a protective, nontoxic coating on the endothelial and epithelial cell linings of kidneys deprived of their GCX due to ischemia. By seamlessly inserting into the cell membrane, it restores the shielding and protective function of the GCX, effectively attenuating IRI *in vivo*.

To demonstrate the effect of PEG-LIPID on IRI, we utilized nonsurvival and survival porcine transplantation models (ANSM, SM1, and SM2), without immunosuppression, monitoring recipients for up to 4 days. Immunosuppressive therapy was excluded to prevent bias from interindividual variability and potential nephrotoxic effects, allowing a controlled investigation of the immediate IRI-driven inflammation. PEG-LIPID-treated

kidneys exhibited significantly reduced innate immune activation compared with untreated kidneys. This was reflected in attenuated plasma levels of biomarkers of the coagulation (TAT and TF), contact (FXIIa-C1INH complexes), and complement (C3a, sC5b-9, including deposited C3 in kidney biopsies) systems. These findings demonstrated that the PEG-LIPID construct effectively inhibited intravascular innate immune system activation after reperfusion of recipient blood, a hallmark of IRI.

Corroborating the results of the immediate inflammation, the later expression of proinflammatory cytokines such as TNF, IL-1 β , and IL-6 was drastically attenuated in PEG-LIPID-treated kidneys across all transplantation models, indicating a markedly lower thromboinflammatory response in the treated group.

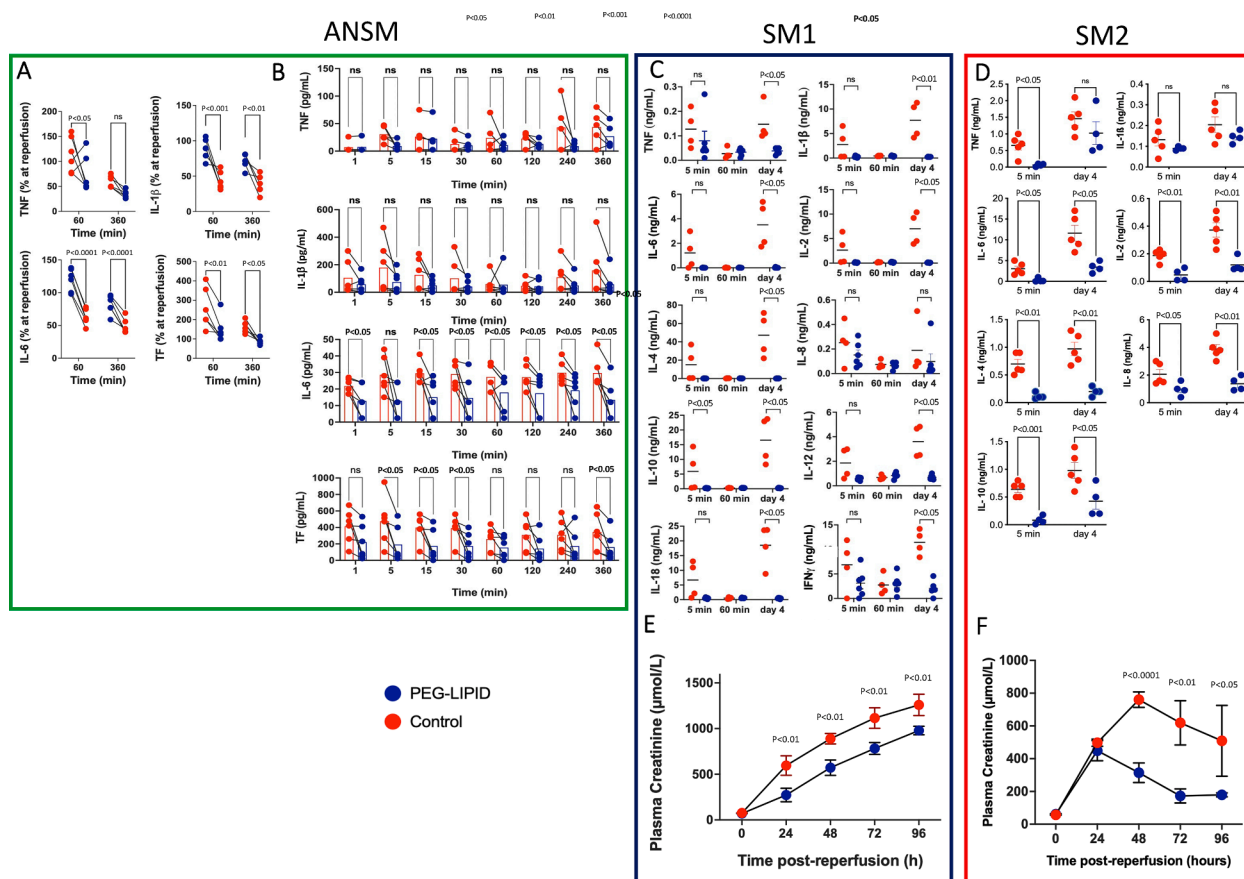


Figure 5. Attenuation of cytokine expression and formation after ex vivo polyethylene glycol-conjugated lipid (PEG-LIPID) treatment of the graft in the porcine transplantation models. (A) Cytokine messenger RNA (mRNA) expression of proinflammatory cytokines and tissue factor (TF) was performed on wedge biopsies from individual kidneys. Cytokine and TF expression were shown to be suppressed throughout the observation period. Results are expressed as a percentage of individual values at reperfusion (5 minutes). (B) Protein levels of proinflammatory cytokines in the ANSM: serial samples from the kidney vein of PEG-LIPID-treated kidneys and their controls were collected for 360 minutes ($n = 6$). (C) Protein levels of cytokines in the survival model (SM)1: cytokines were sampled from the kidney vein of PEG-LIPID-treated kidneys and their controls at 5 and 60 minutes, followed by systemic sampling after 96 hours. By 60 minutes, all cytokines stabilized at a low steady-state level comparable to control values. After 96 hours, all cytokines in treated animals remained suppressed to baseline levels, except for interleukin (IL)-8 and interferon gamma (IFN γ), which were unaffected ($n = 6$ treatments + 4 controls). (D) Protein levels of cytokines in the SM2: plasma were sampled from the kidney vein at 5 minutes and systemically at 4 days. ($n = 5$ treatments + 5 controls). In summary, a significantly lower level of both acute and late inflammation was observed in the ANSM, the SM1, and the SM2 models, reflecting an attenuated ischemia-reperfusion injury (IRI). (E, F) Efficacy of PEG-LIPID ex vivo treatment in kidney transplantation models: kidney function was monitored by plasma creatinine levels before and after transplantation in the SM1 (E) and SM2 (F). Plasma creatinine levels were measured at baseline (pretransplant) and daily at 24, 48, 72, and 96 hours posttransplant. Two-way repeated measure analysis of variance (ANOVA, coated/uncoated).

This effect was particularly pronounced after 4 days in the SMs (SM1 and SM2), where cytokine expression in treated kidneys was very low, whereas in untreated kidneys, most cytokine levels were elevated. The consistent and pronounced inhibition of IL-6 levels serves as an important example. Evidence from clinical trials supports attenuation of IL-6 levels for desensitization and treatment of antibody-mediated rejection in kidney transplantation.³⁰⁻³² The in vivo studies also demonstrated that the effect of PEG-LIPID was associated with improved function in the transplanted kidneys, as reflected in significantly lower creatinine levels in treated kidneys compared with controls in the SMs (SM1 and SM2).

Previous studies have shown that the effect of the PEG-LIPID is mediated by hydrophobic interaction.³³ In vitro, the PEG-LIPID

binding to cells reached saturation after 30 minutes and detached fully after 48 hours. In vivo, in the ANSM, the distribution over a 6-hour posttransplant period was initially more pronounced in the glomeruli and later in the tubular system. In the modified SM, the PEG-LIPID was detected up to 12 to 24 hours after reperfusion and was completely lost after 48 hours. A $t_{1/2}$ of 14 hours was calculated from these studies. Further supporting renal clearance, fluorescence was detected in urine throughout the ANSM observation period.

ROS is an important component of ischemic injury.^{34,35} In our transplantation models, genes involved in ROS metabolism were upregulated, but there was no significant difference in the expression of these genes (nitrotyrosine, HO-1, or inducible nitric oxide synthase) in the PEG-LIPID-treated kidneys compared

with those of the control kidneys in the ANSM. In addition, there was no difference in the morphology between the different groups.³⁶ In vitro cultured cells were not affected by the PEG-LIPID in different experiments investigating, eg, viability, cell proliferation, ADP/ATP ratio, Ca²⁺ flux, etc, demonstrating that the PEG-LIPID is not toxic to the cells. All these results demonstrated that the effect of the PEG-LIPID was not mediated by a direct impact on the ischemic cell phenotype but by the events associated with the reperfusion of the kidney allograft.

The PEG-LIPID treatment constitutes a fundamentally new principle to attenuate IRI in clinical kidney transplantation. Our in vitro data corroborate the concept that the PEG-LIPID (reaching out 6 nm) effectively shields off small surface antigens such as CD52 and the Rh and B antigens, which reach out approximately 1 to 3 nm from the surface.^{23,37} CD8, which ranges between 5 and 10 nm in size,²⁴ and the ligands of lectins (Con A, MBL, and CL-11) are partially blocked, although the PEG-LIPID layer does not block more extended proteins such as CD4 (15 nm),²⁵ CD31 (15 nm),²⁶ and vWF (>100 μm, in a multimeric form).²⁷ These results are compatible with the notion that the PEG-LIPID extends 6 nm out from the cell membrane.^{33,38}

Maximum tissue saturation was found to be 0.3 mg PEG-LIPID/g kidney tissue, administered either by a single arterial infusion or via hypothermic machine perfusion. This saturating dose, reached in SM2, was found to be safe and effective. Comparable efficacy was, however, also observed at lower doses used in ANSM and in SM1 (at the limit of saturation). Furthermore, PEG-LIPID conferred protection regardless of the timing of administration, whether given immediately after kidney recovery (SM2) or at the end of preservation (ANSM and SM1). These findings indicate that PEG-LIPID is effective across a range of doses and administration windows, supporting a flexible and safe dosing strategy.

The distinct efficacy of this novel treatment strategy likely reflects its ability to modulate multiple components of the innate immune system, combining the effects of drugs targeting individual components, such as anti-C5, anti-C3, and C1INH therapies. Safety was also a key focus of our study, where no adverse events, toxicity, or off-target effects were observed in animals treated with PEG-LIPID. In vitro assays further confirmed the absence of effects on cell viability, proliferation, metabolism, or morphology.

This study has limitations. The short observation period and the absence of immunosuppression were deliberately used to isolate early IRI-driven responses but limit conclusions about longer-term outcomes and alloimmunity. Functional assessment focused on local and systemic inflammation, but inclusion of urinary biomarkers, which was hampered by the anatomical and technical restrictions in the current porcine models (see [Supplementary Methods](#)), will strengthen future studies in humans.

Nonetheless, these preclinical studies form the foundation for the first-in-human clinical trial of PEG-lipid (ATMIRE; NCT05246618), currently being evaluated for its safety and tolerability in reducing IRI in diseased-donor kidney transplantation.

In summary, we described a novel ex vivo treatment strategy that uses a fundamentally new modality to reduce IRI in kidney

transplantation. This translational study utilizes PEG-lipid, an amphiphilic polymer designed to create a protective, nontoxic coating on endothelial and tubular cells when infused ex vivo into the vascular tree of the recovered kidney allograft before reperfusion. By effectively attenuating the IRI-induced thromboinflammation and limiting the prolonged systemic inflammation, PEG-LIPID preserves kidney function and provides targeted graft protection from IRI.

Acknowledgments

The authors thank the veterinary pathologists Alexandra Lejon and Lisa Lindqvist for excellent postmortem examinations of the pigs.

Author contributions

A.-R.B., B.N., M.J.-W., and Y.T. were responsible for the study design. Y.T., S.A., F.S., C.D., and V.A.M. performed the in vitro studies and sample analyses. M.J.-W., A.-R.B., S.A., E.M., P.H., A.R., and Y.T. performed the porcine studies. A.-R.B. performed all operation procedures and developed the ANSM model. S.H. was responsible for SLA-typing determinations, and M.H.-L. for immunohistochemical analyses. B.N., K.N.E., C.D., and K.F. compiled and validated all data. B.N. was the project coordinator and main contributor to manuscript writing together with A.-R.B., M.J.-W., Y.T., and K.N.E. All authors read and approved the final version of the manuscript.

Funding

This work was supported by the European Community's Seventh Framework Programme under the grant agreement no. 602699 (DIREKT), the Swedish Research Council (VR) grants 2016-01060, 2016-04519, 2020-05762, 2021-02252, the Swedish Foundation for International Cooperation in Research and Higher Education (STINT), the Bilateral Joint Research Projects (Japan-Sweden) of the Japan Society for the Promotion of Science (JSPS), Grant-in-Aid for Scientific Research for Fostering Joint International Research (18KK0305) from the Ministry of Education Culture Sports Science and Technology (MEXT) of Japan, and faculty grants from the Linnæus University.

Declaration of competing interest

The authors of this manuscript have conflicts of interest to disclose as described by *American Journal of Transplantation*. Based on the results from this study, B. Nilsson, M. Jensen-Waern, A.-R. Biglarnia, K.N. Ekdahl, and Y. Teramura founded iCoat Medical AB. They are all shareholders in the company and inventors of patents owned by iCoat Medical AB. No consultancy fees or other remuneration have been received. V.A. Manivel and C. Dührkop were researchers at Uppsala University, later investigators at iCoat Medical AB. The other authors of this manuscript have no conflicts of interest to disclose as described by *American Journal of Transplantation*.

Data availability

All essential data are presented in the article. In addition to primary research data, we will share other materials and resources related to the article as far as possible. There are no large data files to be shared via online resources.

Appendix A. Supplementary data

Supplementary data to this article can be found online at <https://doi.org/10.1016/j.ajt.2025.08.024>.

ORCID

Ali-Reza Biglarnia  <https://orcid.org/0009-0004-2293-0740>
 Yuji Teramura  <https://orcid.org/0000-0002-0709-1000>
 Sana Asif  <https://orcid.org/0000-0001-7924-0936>
 Claudia Dührkop  <https://orcid.org/0009-0006-9405-4035>
 Vivek Anand Manivel  <https://orcid.org/0000-0002-6746-7372>
 Elin Manell  <https://orcid.org/0000-0002-4491-7609>
 Patricia Hedenqvist  <https://orcid.org/0000-0003-4540-6250>
 Anneli Rydén  <https://orcid.org/0000-0002-3070-5023>
 Felix Sellberg  <https://orcid.org/0000-0002-9742-244X>
 Karin Fromell  <https://orcid.org/0000-0001-8905-8791>
 Sabine Hammer  <https://orcid.org/0000-0003-1475-3938>
 Markus Huber-Lang  <https://orcid.org/0000-0003-2359-6516>
 Kristina N. Ekdahl  <https://orcid.org/0000-0001-7888-1571>
 Marianne Jensen-Waern  <https://orcid.org/0000-0001-6195-7066>
 Bo Nilsson  <https://orcid.org/0000-0003-0057-2730>

References

- Ko DSC. Reducing ischemia-reperfusion injury in renal transplantation. *J Urol*. 2015;194(6):1531–1532. <https://doi.org/10.1016/j.juro.2015.09.060>.
- Kluge KE, Langseth MS, Opstad TB, et al. Complement activation in association with markers of neutrophil extracellular traps and acute myocardial infarction in stable coronary artery disease. *Mediators Inflamm*. 2020;2020:5080743. <https://doi.org/10.1155/2020/5080743>.
- Li MT, Ramakrishnan A, Yu M, et al. Effects of delayed graft function on transplant outcomes: a meta-analysis. *Transplant Direct*. 2023;9(2):e1433. <https://doi.org/10.1097/TXD.0000000000001433>.
- Moore KH, Murphy HA, George EM. The glycocalyx: a central regulator of vascular function. *Am J Physiol Regul Integr Comp Physiol*. 2021;320(4):R508–R518. <https://doi.org/10.1152/ajpregu.00340.2020>.
- Möckl L. The emerging role of the mammalian glycocalyx in functional membrane organization and immune system regulation. *Front Cell Dev Biol*. 2020;8:253. <https://doi.org/10.3389/fcell.2020.00253>.
- Reitsma S, Slaaf DW, Vink H, van Zandvoort MA, oude Egbrink MG. The endothelial glycocalyx: composition, functions, and visualization. *Pflugers Arch*. 2007;454(3):345–359. <https://doi.org/10.1007/s00424-007-0212-8>.
- Ekdahl KN, Teramura Y, Hamad OA, et al. Dangerous liaisons: complement, coagulation, and kallikrein/kinin cross-talk act as a linchpin in the events leading to thromboinflammation. *Immunol Rev*. 2016;274(1):245–269. <https://doi.org/10.1111/imir.12471>.
- Slegtenhorst BR, Dor FJMF, Rodriguez H, Voskuil FJ, Tullius SG. Ischemia/reperfusion injury and its consequences on immunity and inflammation. *Curr Transplant Rep*. 2014;1(3):147–154. <https://doi.org/10.1007/s40472-014-0017-6>.
- Farrar CA, Sacks SH. Mechanisms of rejection: role of complement. *Curr Opin Organ Transplant*. 2014;19(1):8–13. <https://doi.org/10.1097/MOT.000000000000037>.
- Farrar CA, Zhou W, Sacks SH. Role of the lectin complement pathway in kidney transplantation. *Immunobiology*. 2016;221(10):1068–1072. <https://doi.org/10.1016/j.imbio.2016.05.004>.
- Orsini F, Chrysanthou E, Dudler T, et al. Mannan binding lectin-associated serine protease-2 (MASP-2) critically contributes to post-ischemic brain injury independent of MASP-1. *J Neuroinflammation*. 2016;13(1):213. <https://doi.org/10.1186/s12974-016-0684-6>.
- Tillet S, Giraud S, Delpech PO, et al. Kidney graft outcome using an anti-Xa therapeutic strategy in an experimental model of severe ischaemia-reperfusion injury. *Br J Surg*. 2015;102(1):132–142. discussion 142. <https://doi.org/10.1002/bjs.9662>.
- Strandberg G, Öberg CM, Blom AM, et al. Prompt thrombo-inflammatory response to ischemia-reperfusion injury and kidney transplant outcomes. *Kidney Int Rep*. 2023;8(12):2592–2602. <https://doi.org/10.1016/j.ekir.2023.09.025>.
- Tatsumi K, Ohashi K, Teramura Y, et al. The non-invasive cell surface modification of hepatocytes with PEG-lipid derivatives. *Biomaterials*. 2012;33(3):821–828. <https://doi.org/10.1016/j.biomaterials.2011.10.016>.
- Teramura Y, Iwata H. Improvement of graft survival by surface modification with poly(ethylene glycol)-lipid and urokinase in intraportal islet transplantation. *Transplantation*. 2011;91(3):271–278. <https://doi.org/10.1097/tp.0b013e3182034fa4>.
- Teramura Y, Iwata H. Islets surface modification prevents blood-mediated inflammatory responses. *Bioconjugate Chem*. 2008;19(7):1389–1395. <https://doi.org/10.1021/bc800064t>.
- Nilsson B, Larsson R, Hong J, et al. Compstatin inhibits complement and cellular activation in whole blood in two models of extracorporeal circulation. *Blood*. 1998;92(5):1661–1667.
- Nilsson Ekdahl K, Nilsson B, Pekna M, Nilsson UR. Generation of iC3 at the interface between blood and gas. *Scand J Immunol*. 1992;35(1):85–91. <https://doi.org/10.1111/j.1365-3083.1992.tb02837.x>.
- Rydén A, Manell E, Biglarnia A, et al. Nursing and training of pigs used in renal transplantation studies. *Lab Anim*. 2020;54(5):469–478. <https://doi.org/10.1177/0023677219879169>.
- Hammer SE, Ho CS, Ando A, et al. Importance of the major histocompatibility complex (Swine leukocyte antigen) in Swine health and biomedical research. *Annu Rev Anim Biosci*. 2020;8(1):171–198. <https://doi.org/10.1146/annurev-animal-020518-115014>.
- Hammer SE, Duckova T, Groiss S, et al. Comparative analysis of swine leukocyte antigen gene diversity in European farmed pigs. *Anim Genet*. 2021;52(4):523–531. <https://doi.org/10.1111/age.13090>.
- Hammer SE, Duckova T, Gociman M, et al. Comparative analysis of swine leukocyte antigen gene diversity in Göttingen Minipigs. *Front Immunol*. 2024;15:1360022. <https://doi.org/10.3389/fimmu.2024.1360022>.
- Avent ND, Reid ME. The Rh blood group system: a review. *Blood*. 2000;95(2):375–387. <https://doi.org/10.1182/blood.v95.2.375>.
- Leahy DJ, Axel R, Hendrickson WA. Crystal structure of a soluble form of the human T cell coreceptor CD8 at 2.6 Å resolution. *Cell*. 1992;68(6):1145–1162. [https://doi.org/10.1016/0092-8674\(92\)90085-q](https://doi.org/10.1016/0092-8674(92)90085-q).
- Yin Y, Wang XX, Mariuzza RA. Crystal structure of a complete ternary complex of T-cell receptor, peptide-MHC, and CD4. *Proc Natl Acad Sci U S A*. 2012;109(14):5405–5410. <https://doi.org/10.1073/pnas.1118801109>.
- Liu L, Shi GP. CD31: beyond a marker for endothelial cells. *Cardiovasc Res*. 2012;94(1):3–5. <https://doi.org/10.1093/cvr/cvs108>.
- Michaux G, Abbitt KB, Collinson LM, Haberichter SL, Norman KE, Cutler DF. The physiological function of von Willebrand's factor depends on its tubular storage in endothelial weibel-palade bodies. *Dev Cell*. 2006;10(2):223–232. <https://doi.org/10.1016/j.devcel.2005.12.012>.
- Rowan WC, Hale G, Tite JP, Brett SJ. Cross-linking of the CAMPATH-1 antigen (CD52) triggers activation of normal human T lymphocytes. *Int Immunol*. 1995;7(1):69–77. <https://doi.org/10.1093/intimm/7.1.69>.

29. Qi R, Qin W. Role of complement system in kidney transplantation: stepping from animal models to clinical application. *Front Immunol.* 2022;13:811696. <https://doi.org/10.3389/fimmu.2022.811696>.
30. Miller CL, Madsen JC. IL-6 directed therapy in transplantation. *Curr Transplant Rep.* 2021;8(3):191–204. <https://doi.org/10.1007/s40472-021-00331-4>.
31. Shen H, Goldstein DR. IL-6 and TNF- α synergistically inhibit allograft acceptance. *J Am Soc Nephrol.* 2009;20(5):1032–1040. <https://doi.org/10.1681/ASN.2008070778>.
32. Jordan SC, Choi J, Kim I, et al. Interleukin-6, a cytokine critical to mediation of inflammation, autoimmunity and allograft rejection: therapeutic implications of IL-6 receptor blockade. *Transplantation.* 2017;101(1):32–44. <https://doi.org/10.1097/TP.0000000000001452>.
33. Sou K, Endo T, Takeoka S, Tsuchida E. Poly(ethylene glycol)-modification of the phospholipid vesicles by using the spontaneous incorporation of poly(ethylene glycol)-lipid into the vesicles. *Bioconjugate Chem.* 2000;11(3):372–379. <https://doi.org/10.1021/bc990135y>.
34. Raedschelders K, Ansley DM, Chen DDY. The cellular and molecular origin of reactive oxygen species generation during myocardial ischemia and reperfusion. *Pharmacol Ther.* 2012;133(2):230–255. <https://doi.org/10.1016/j.pharmthera.2011.11.004>.
35. Wagner M, Cadetg P, Ruf R, Mazzucchelli L, Ferrari P, Redaelli CA. Heme oxygenase-1 attenuates ischemia/reperfusion-induced apoptosis and improves survival in rat renal allografts. *Kidney Int.* 2003;63(4):1564–1573. <https://doi.org/10.1046/j.1523-1755.2003.00897.x>.
36. Stubenitsky BM, Booster MM, Brasile L, et al. II: ex vivo viability testing of kidneys after postmortem warm ischemia. *ASAIO J.* 2000;46(1):62–64. <https://doi.org/10.1097/00002480-200001000-00017>.
37. Cheetham GM, Hale G, Waldmann H, Bloomer AC. Crystal structures of a rat anti-CD52 (CAMPATH-1) therapeutic antibody Fab fragment and its humanized counterpart. *J Mol Biol.* 1998;284(1):85–99. <https://doi.org/10.1006/jmbi.1998.2157>.
38. Kenworthy AK, Hristova K, Needham D, McIntosh TJ. Range and magnitude of the steric pressure between bilayers containing phospholipids with covalently attached poly(ethylene glycol). *Biophys J.* 1995;68(5):1921–1936. [https://doi.org/10.1016/S0006-3495\(95\)80369-3](https://doi.org/10.1016/S0006-3495(95)80369-3).